IEICE TRANS. COMMUN., VOL.E82–B, NO.10 OCTOBER 1999

LETTER

Application of Mix-Phase Wavelets to Sparsify Impedance Matrices

Jiunn-Ming HUANG[†], **Jeng-Long LEOU**[††], **Shyh-Kang JENG**[††], *and* **Jenn-Hwan TARNG**[†], ***Nonmembers***

SUMMARY Effective wavelets to solve electromagnetic integral equations are proposed. It is based on the same construction procedure as Daubechies wavelets but with mix-phase to obtain maximum sparsity of moment matrix. These new wavelets are proved to have excellent performance in non-zero elements reduction in comparison with minimum-phase wavelet transform (WT). If further sparsity is concerned, wavelet packet (WP) transform can be applied but increases the computational complexity. In some cases, the capability of non-zero elements reduction by this new wavelets even better than WP with minimum-phase wavelets and with less computational efforts. Numerical experiments demonstrate the validity and effectiveness of the new wavelets.

key words: *electromagnetic scattering, mix-phase wavelet, impedance matrices*

1. Introduction

In computational electromagnetics, method of moments (MoM) is a well-established technique but produces a dense impedance matrix and becomes the major drawback. Recently, the use of wavelets for the solution of electromagnetic (EM) integral equations (IE) receives more attentions [1]–[10]. The term 'wavelet' was introduced by Grossman and Morlet [11] to describe a square integrable function, appropriate translations and dilations of which form a basis for $L^2(\mathbb{R})$. The most salient features of wavelets are sparse matrix can be obtained. Because a classical basis function contains only magnitude/phase information while the wavelet is constructed not only magnitude/phase but also frequency (scale) information. Beylkin et al. [9], [10] first applied wavelets to the solution of IE having smooth kernels (similar to those in electrostatic case). For such problems, wavelets can be used to obtain a solution in $O(N \log N)$ operations, where N is the number of unknowns in the discretized IE. However, the kernel of IE in electrodynamics is an oscillatory type. Wavelets do not produce as dramatic a saving as for smooth kernels. Most of the studies never pinpoint which kind of wavelets is more suitable to EM IE with oscillatory kernels. Many papers use Daubechies minimum-phase wavelets to obtain sparsification of matrix in MoM, but the discretionary choice of wavelets will need more expensive algorithm such as wavelet packet (WP) [2] to further sparsify the matrix. It is because that the wavelets are originally designed for the purpose of signal/image processing. A more specialized wavelets should be constructed to efficiently solve EM IE with oscillatory kernels and to fully capitalize the potential of the wavelet representation.

This paper propose an alternative construction scheme based on the same procedure as developed by Daubechies [12], [13] but choose mix-phase wavelets instead of minimum-phase ones. The non-zero elements reduction by the new wavelets cannot be achieved with conventional minimum-phase wavelets. In Sect. 4, numerical results are presented to demonstrate the validity and effectiveness of the new wavelets.

2. Wavelet Transformation and Wavelet Construction

Many EM problems can be formulated as the form of inhomogeneous equation

$$\mathcal{L}f = g \tag{1}$$

where $\mathcal{L}$ is a linear operator, g is a known excitation and f is to be determined.

MoM can be used to solve Eq. (1). After expansion of the unknown function in terms of N known basis and weighting procedure, the algebraic linear equation systems can be obtained as

$$\mathbf{Z}\,\mathbf{I} = \mathbf{V} \tag{2}$$

The discrete wavelet transform of a discrete signal is the signal multiplied by a unitary matrix. The unitary matrix arises from a wavelet basis for $L^2(\mathbb{R})$ in a manner which is addressed at the following of this section. Let W be a unitary wavelet matrix of order $N \times N$, the wavelet domain equation is formed as

$$\tilde{\mathbf{Z}}\,\tilde{\mathbf{I}} = \tilde{\mathbf{V}} \tag{3}$$

where $\tilde{Z} = WZW^T, \tilde{V} = WV$ and $\tilde{I} = (W^T)^{-1}I$

Although the wavelet has no explicit analytic form, it can be obtained through the scaling function coefficients. The scaling function and wavelet function are

Manuscript received February 16, 1999.
Manuscript revised May 29, 1999.

[†]The authors are with the Department of Communication Engineering, National Chiao-Tung University, Hsinchu, Taiwan, Republic of China.
[††]The authors are with the Department of Electrical Engineering, National Taiwan University, Taipei, Taiwan, Republic of China.

defined as follows [12]:

$$\Phi(x) = \sqrt{2}\sum h_n \Phi(2x-n) \tag{4}$$

$$\Psi(x) = \sqrt{2}\sum g_n \Phi(2x-n) \tag{5}$$

$$g_n = (-1)^{1-n} h_{1-n}, n \in \mathbb{Z} \tag{6}$$

where h_n and g_n are the coefficients of scaling and wavelet functions. The wavelet coefficients g_n is chosen to have certain number of vanishing moments ν_m.

$$\sum_{n=1}^{2\nu_m+1} n^j g_n = 0, \qquad j = 0, \cdots, \nu_m - 1 \tag{7}$$

In order to compare different orthogonal wavelets, the W matrix must be implemented quickly. For a vector s^0 of size $N = 2^n$, a $N \times N$ matrix W_n is decomposed as

$$W_n = \begin{bmatrix} H_n \\ G_n \end{bmatrix}$$

where H_n and G_n are matrices of order $2^{n-1} \times 2^n$ called the low- and high-pass filters, respectively. For example $\nu_m = 2$

$$H_n = \begin{bmatrix} h_1 & h_2 & h_3 & h_4 & 0 & \cdots & & 0 \\ 0 & 0 & h_1 & h_2 & h_3 & h_4 & \cdots & 0 \\ \vdots & \vdots & & & \ddots & & \vdots & \vdots \\ 0 & \cdots & & & h_1 & h_2 & h_3 & h_4 \\ h_3 & h_4 & \cdots & & & & h_1 & h_2 \end{bmatrix} \tag{8}$$

$$G_n = \begin{bmatrix} g_1 & g_2 & g_3 & g_4 & 0 & \cdots & & 0 \\ 0 & 0 & g_1 & g_2 & g_3 & g_4 & \cdots & 0 \\ \vdots & \vdots & & & \ddots & & \vdots & \vdots \\ 0 & \cdots & & & g_1 & g_2 & g_3 & g_4 \\ g_3 & g_4 & \cdots & & & & g_1 & g_2 \end{bmatrix} \tag{9}$$

The filter coefficients are wrapped around to form a circulant matrix. $W_n s^0$ decompose s^0 into smooth (average) part s^1 and detail (difference) part d^1.

Continuing the process of recursive decomposition of smooth vectors $s^j, j = 1, \cdots, \ell \leq n - \log_2 2\nu_m + 1$, we obtain the discrete wavelet transform of the vector s^0. In matrix notation, $Ws^0 = W_{n-\ell} \cdots W_{n-1} W_n s^0 = [s^\ell, d^\ell, \cdots, d^1]$ and W_{n-j} is a block-diagonal matrix of the form

$$W_{n-j} = \begin{bmatrix} \begin{bmatrix} H_n \\ G_n \end{bmatrix} & 0 \\ 0 & I_{N-N/2^j} \end{bmatrix}$$

where $I_{N-N/2^j}$ is the identity matrix of rank $N - N/2^j$.

W matrix can be implemented to a MATLAB function as following:

```
function    W=W_matrix(Coefficients,N)
number=\log2(N);
m=sparse(eye(N));
a=sparse(eye(N));
index=N/2^(number);
while index<=N/2
a(1:2*index,1:2*index)=sparse
(Block_matrix(Coefficients,2*index));
m=a*m;
index=2*index;
end
W=sparse(m);
```

We can construct the coefficients h_n by the same procedure as developed by Daubechies. The discrete Fourier transform of h_n has K zeros at $\omega = \pi$ of the form

$$H(\omega) = \left(\frac{1+e^{i\omega}}{2}\right)^K L(\omega) \tag{10}$$

satisfies

$$|H(\omega)|^2 + |H(\omega+\pi)|^2 = 2 \tag{11}$$

The steps in calculating the actual values of h_n are to first choose the filter length N_L or vanishing moment ν_m for h_n, then factor $|H(\omega)|^2$ where there will be freedom in choosing which roots to use for $|H(\omega)|$. Conventionally, a different set of $\nu_m - 1$ roots is chosen to get a minimum-phase (all roots are inside a unit circle) or maximum-phase (outside a unit circle). In this paper, we proposed to use even mix-phase, that means some roots are inside a unit circle and the others are outside the circle. It is found that using suitable root sets can results in more matrix sparsity than the original minimum-phase wavelet for every IE in EM applications.

The mix-phase wavelets which maxmize the sparsity of moment matrix is obtained using the following steps:

1. Given a vanishing moment ν_m or filter length N_L.
2. Construct a small size (for example, $N = 64$ or $N = 32$) linear system equation with fixed discretization size.
3. Combining all possible roots which satisfy $\sum h_n = \sqrt{2}$ and $norm(h_n) = 1$.
4. Fast construction of W matrix with the new mix-phase wavelet coefficients and use it to transform the small size linear system equation in step 2.
5. Go to step 3 with another wavelets.
6. Select the wavelet with maximum sparsity of moment matrix.

Theoretically, there are $C(N_L, N_L/2)$ selections to find the best wavelet, and it seems a time-consuming task. In this paper we have proposed new wavelets, although they may be not the best, however, they can

improve significantly the sparsity of the impedance matrix for 2D scatterers. In our approach, there are two major reasons that can reduce the number of selections tremendously and they lead to determine suitable N_L easily. These two reasons are given as following:
(1) Satisfaction of $\sum h_n = \sqrt{2}$ and $norm(h_n) = 1$ greatly reduce the number of selections.
(2) The larger N_L is chosen, the higher compression rate of the matrix is [5]. From our numerical experiments, we find an interesting fact that after N_L is larger than a certain value, the increase rate of sparsity is negligible small, i.e., it is saturated. This fact is confirmed in Sarkar's paper [7]. Therefore, the suitable value of N_L is easily found.

The new wavelet constructed for a small size target can also apply to the same application with a large size.

3. Wavelet Packet

The WT tree follows the rigid constant-Q structure that zooms in progressively onto the lowest spectral content. However, at each decomposition level two branches are possible. Either low-frequency or high-frequency or only high-frequency can be decomposed. By adaptively selecting transformation bases based on a cost function at every node of the decomposition, the wavelet packet (WP) transform can be applied to sparsify the impedance matrix. Note that the transformation matrix in any cases is still orthogonal.

Many different types of basis selection algorithm (top-down or bottom-up) and cost functions (entropy, log-energy or ℓ^p norm) can be chosen in WP. For verification of the new wavelets, we adopted the same scheme as [2]. Starting with the incident wave vector as the top node of WP decomposition tree, a decision whether to continue decomposition or not is based on the norms of vectors between any given node and its two descendants. A branch stops growing as long as the cost of the descendants is greater than its own cost. The information cost function used as a criterion is

$$\mathcal{C}(x) = \sum_i |x_i|, x = [x_1, x_2, \cdots, x_M]^t \tag{12}$$

where x is a vector of transform coefficients related to the node.

Since this top-down algorithm may not expand the full tree, it does not guarantee finding the best tree for the given incident vector and cost. The selected basis is a near-best tree. If the best basis selection is concerned, the searching time will increase. The effect of basis selection algorithm and cost function is beyond our discussion. Our focus is to evaluate performance of different wavelets using the same WP algorithm.

Once the tree structure has been determined, the associated W matrix is obtained and applied to matrix Z. The remaining procedure is the same as WT. The same steps can be applied to our problems with many

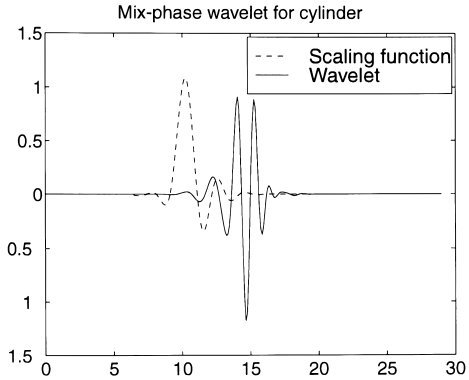

Fig. 1 Mix-phase wavelet h_{cyl} for cylindrical scatterer.

excitation and the cost function is modified as [2]:

$$\mathcal{C}(x) = \sum_j \sum_i |x_i^{(j)}|, x = \begin{bmatrix} x_1^{(1)} & \cdots & x_1^{(m)} \\ \vdots & \ddots & \vdots \\ x_M^{(1)} & \cdots & x_M^{(m)} \end{bmatrix} \tag{13}$$

4. Numerical Results

In this section we use the fast construction method in section II and WP in section III to solve EM scattering IE. To compare with other published results, a two dimensional (2D) L-shape scatterer and cylinder are chosen to validate the proposed wavelets using the same discretization size (10 points per λ) and relative residual error. A discretization size of 0.1λ is often sufficient for modelling the current on the scatterer. If finer discretization were used, the greater sparsity is obtained but at the cost of more unknowns for a given problem. Detail explanations can be found in [1], [4]. By changing the physical size of the scatterer proportionally, the MoM matrices with sizes ranging from $N = 256$ to 2048 are obtained. The relative residual error is defined by

$$\text{Residual error} = \frac{||\tilde{V} - \tilde{Z}\tilde{J}_c||}{||\tilde{V}||} \times 100\% \tag{14}$$

where $\tilde{J}_c$ is determined from thresheld matrix $\tilde{Z}$. Here we fix the residual error at $(1 \pm 0.1)\%$.

Consider the problem of computing the scattering of a $TM(E_z)$ polarized EM wave from a 2D conducting scatterer. The scattering characteristics are obtained from the surface current density J_z excited by an incident wave E_z^{inc}. An electric field integral equation is obtained by enforcing the boundary condition that $E_z = 0$ on the conductor.

$$\oint_c J_z(r')\ G(r, r')\ dr' = -E_z^{inc}(r) \tag{15}$$

where c represents the surface of the scatterer.

Equation (15) is discretized by MoM into an algebraic linear system equation. We constructed two wavelets as shown in Figs. 1 and 2 for a cylindrical scatterer (h_{cyl}) and a L-shape scatterer (h_L) ,respectively.

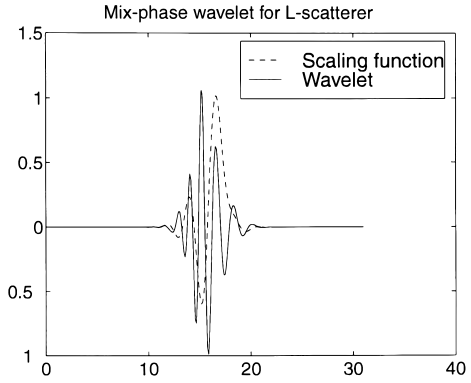

Fig. 2 Mix-phase wavelet h_L for L-shape scatterer.

Table 1 Mix-phase wavelets h_{cyl} and h_L.

h_{cyl} $N = 30$	h_L $N = 32$
0.00012064240013	-0.00000462293728
0.00048653726272	-0.00000183089979
-0.00086660717279	0.00008997332343
-0.00730267579582	0.00005535444015
-0.01010291977672	-0.00079642397562
0.00577918215105	-0.00058189688878
0.00709541319204	0.00463149118922
-0.04580099730228	0.00441785814370
-0.00801537800823	-0.01893401796669
0.32415943648389	-0.02661457049317
0.70151492975568	0.04560810630333
0.58184441633955	0.09597706335602
0.05113673481164	-0.07106173821524
-0.21517222389064	-0.29875833882473
-0.04937695729375	-0.14154555199946
0.09168376863559	0.37414948758196
0.02367122719618	0.66668993199422
-0.03719361387820	0.48896576825320
-0.00982995755255	0.20107582421104
0.01080769446780	0.08176890869036
0.00187457897073	0.04363525122296
-0.00259337625278	-0.00386462380391
-0.00007580194258	-0.02313096870950
0.00044450388123	-0.00843097593427
-0.00005283597558	0.00164346970142
-0.00003439553830	-0.00003600697420
0.00001516971040	-0.00107992018032
-0.00000191053961	0.00000636863850
-0.00000145712805	0.00030827729177
0.00000043516234	0.00006068793856
	-0.00002230006675
	-0.00000647203702

The wavelet coefficients are found and listed in Table 1.

Figures 1 and 3 show that the differences between a minimum-phase wavelet and a mix-phase wavelet for a cylindrical scatterer. We note that the new wavelet and scaling function are more localized at center of their support. However, Daubechies wavelets are very asymmetric because they are constructed by selecting minimum-phase roots of Eq. (10). One can show that filters corresponding to a minimum-phase square root have their energy concentrated near the starting point of their support [14]. Similar result is observed for a L-shape scatterer after comparing Fig. 2 with Fig. 4.

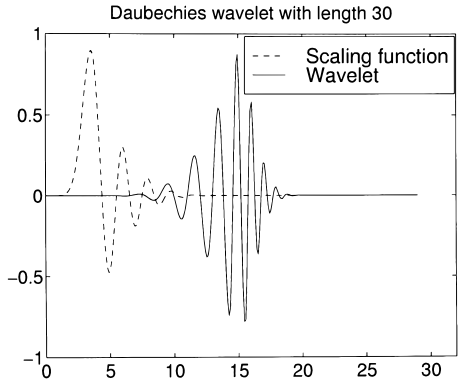

Fig. 3 Daubechies minimum-phase wavelet with filter length 30.

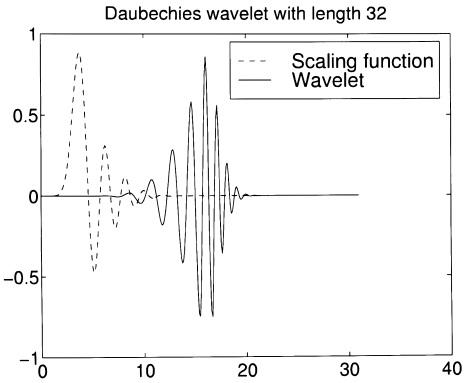

Fig. 4 Daubechies minimum-phase wavelet with filter length 32.

Figures 5 and 6 show the induced surface current, which are computed by the proposed WT MoM and MoM, for a cylinder and a L-shape scatterers, respectively. From each figure it is found that the solution accuracy between MoM and the proposed WT MoM is almost the same when the residual error is fixed at 1%. The value of residual error is acceptable and widely adopted in the society. The values between MoM and exact solution is practically indistinguishable in Fig. 5. The exact solution for cylindrical scatterer is given by [15]:

$$J_z = \frac{-2E_0}{\omega\mu\pi a} \sum_{n=-\infty}^{\infty} \frac{\jmath^{-n} e^{\jmath n\phi}}{H_n^{(2)}(ka)}$$

where $n = 300$ in numerical computation because the magnitude for $n > 300$ is negligible small.

Figures 7 and 8 are the images of non-zero elements using the proposed wavelets. To compare with [1], it is obvious that the non-zero elements in finger-band (off-diagonal blocks) of Fig. 7 is drastically reduced for the cylinder case. The same result is also illustrated in Fig. 8. This means that the interaction between new wavelet basis functions on different resolution levels is smaller than the minimum-phase ones.

The percent of non-zero elements as a function of

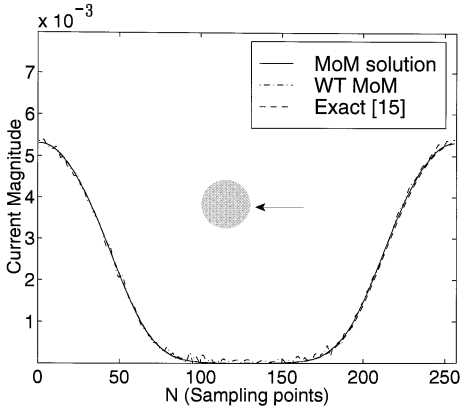

Fig. 5 Induced surface current for a cylinder with $ka = 25.6, N = 256$.

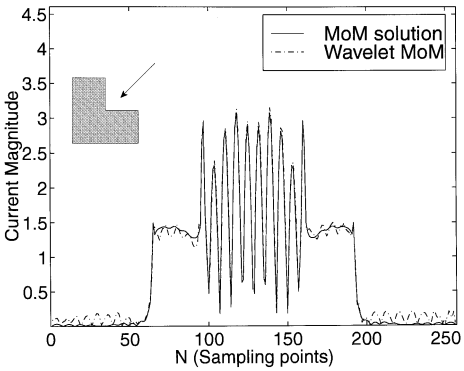

Fig. 6 Induced surface current for a L-shape scatterer with $contour = 25.6\lambda, N = 256$.

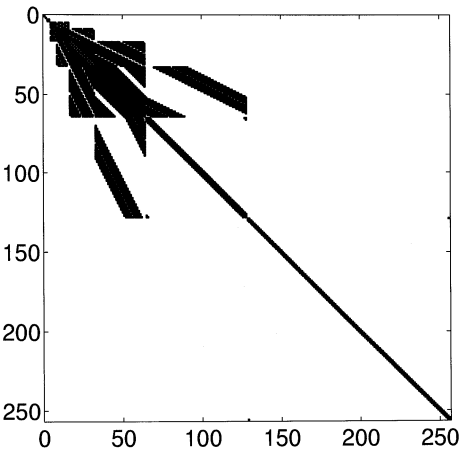

Fig. 7 Non-zero elements of wavelet moment matrix after thresholding for a cylinder with $ka = 25.6, N = 256$.

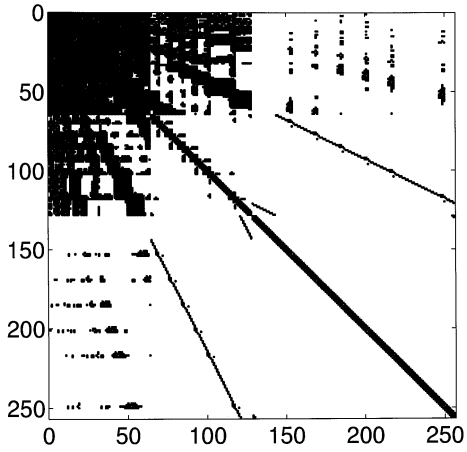

Fig. 8 Non-zero elements of wavelet moment matrix after thresholding for a L-shape scatterer with $contour = 25.6\lambda, N = 256$.

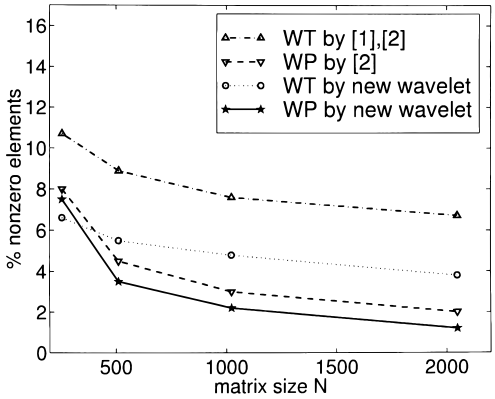

Fig. 9 Matrix sparsity as a function of matrix size N by different methods for a cylindrical scatterer.

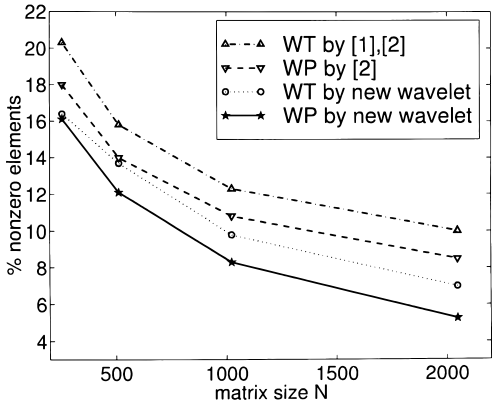

Fig. 10 Matrix sparsity as a function of matrix size N by different methods for L-shaped scatterer.

matrix size N by new wavelets and published data [1], [2] are shown in Figs. 9 and 10 for the cylinder and the L-shape scatterer, respectively. Here WP with a block incident vectors with evenly spaced angles is applied to L-shape scatterer. From these figures we note that, the new wavelets always have smaller percentage than minimum-phase WT and WP.

As shown by Fig. 9, the sparsity drops slowly for

large N in the cylinder case. Hence, another wavelet design for cylindrical scatterer is needed because the sparsity is only a weak function of problem size. However, the sparsity changes faster in the L-shape scatterer because the relative importance of corners diminishes. The results suggest that the choice of wavelet is important for fast solution of IE. Suitable choice does not need WP to further sparsify the moment matrix. If more sparsity is interested, new wavelets design, basis selection scheme and cost function definition offer a promising direction to study.

5. Conclusion

New wavelets have been applied to the IE solution of 2D EM scattering problems. Comparing with published data, these new wavelets are proved to have excellent performance in non-zero elements reduction in comparison with the celebrated Daubechies wavelets. What kind of wavelet is more effective to EM IE needs further study. A more efficient set of wavelet bases should be constructed in order to fully capitalize the potential of wavelets. It is found that some wavelets construction methods in signal/image processing may have good performance in the applications of EM IE problems. These results will be published in the near future. How to correlate the wavelets in filter design and their applications in EM IE is an interesting area of research. Its further development may contribute to the improvement of the computational EM codes.

References

[1] R.L. Wagner and W.C. Chew, "A study of wavelets for the solution of electromagnetic integral equations," IEEE Trans. Antennas & Propag., vol.43, pp.802–810, Aug. 1995.

[2] W.L. Golik, "Wavelet packets for fast solution of electromagnetic integral equations," IEEE Trans. Antennas & Propag., vol.46, no.5, pp.618–624, May 1998.

[3] B.Z. Steinberg and Y. Leviatan, "On the use of wavelet expansions in the method of moments," IEEE Trans. Antennas & Propag., vol.41, pp.610–619, May 1993.

[4] H. Kim and H. Lin, "On the application of fast wavelet transform to the integral equation solution of electromagnetic scattering problems," Microwave Opt. Technol. Lett., vol.6, no.3, pp.168–173, 1993.

[5] Z. Xiang and Y. Lu, "An effective wavelet matrix transform approach for efficient solutions of electromagnetic integral equations," IEEE Trans. Antennas & Propag., vol.45, no.8, pp.1205–1213, Aug. 1997.

[6] G. Wang, "On the utilization of periodic wavelet expansions in moment methods," IEEE Trans. Microwave Theory & Tech., vol.43, pp.2495–2498, Oct. 1995.

[7] T.K. Sarkar, et al. "A tutorial on wavelets from an electrical engineering perspective, Part 1: Discrete wavelet transform," IEEE Antennas and Propagation Magazine., vol.40, no.5, pp. 49–70, Oct. 1998.

[8] G. Pan, "Orthogonal wavelets with applications in electromagnetics," IEEE Trans. Magn., vol.32, pp.975–982, May 1996.

[9] G. Beylkin, R. Coifman, and V. Rokhlin, "Fast wavelet transforms and numerical algorithms I," Commun. Pure Appl. Math., vol.44, pp.141–183, 1991.

[10] B. Alpert, G. Beylkin, R. Coifman, and V. Rokhlin, "Wavelet-like bases for the fast solution of second-kind integral equations," SIAM J. Sci. Comput., vol.14, no.1, pp.159–184, Jan. 1993.

[11] A. Grossman and J. Morlet, "Decomposition of Hardy functions into square integrable wavelets of constant shapes," SIAM J. Math. Anal., vol.15, pp.723–736, 1984.

[12] I. Daubechies, Ten Lectures on Wavelets, CBMS Lecture Notes, SIAM, Philadelphia, PA, 1992.

[13] G. Strang and T. Nguyen, Wavelets and Filter Banks, Wellesley-Cambridge Press, Wellesley, MA, 1996.

[14] A.V. Oppenheim and R.W. Shafer, Discrete-Time Signal Processing, Prentice-Hall, Englewood Cliffs, NJ, 1989.

[15] R.F. Harrington, Time-Harmonic Electromagnetic Fields, McGraw-Hill, New York, 1961.